FUNDAMENTAL RESEARCH

For. Sci. 63(4):362–376
https://doi.org/10.5849/FS-2016-064R1

forest management

Finite Element Analysis to Predict In-Forest Stored Harvest Residue Moisture Content

Francisca Belart, Ben Leshchinsky, and John Sessions

Numerous researchers have worked on measuring and predicting wood moisture content to increase wood's economic value for bioenergy production. Most have focused on small logs, and predicting models include methods such as heuristic fitting and multiple regression. Finite element analysis (FEA) is a method that allows determining drying rates while offering the flexibility of changing the way these residues are stored and their shape and location, material properties, and drying seasons. FEA was used to develop drying rates for four different Oregon climate regions including Willamette Valley (Douglas-fir), higher elevation Douglas-fir, Coast (Western hemlock), and East (Ponderosa pine). Compared with field data, statistical tests show model agreement with correlations between 0.56 and 0.92 in all sites. After performing analyses, we can conclude that selection of pile shape or size can be beneficial or detrimental toward drying, depending on ambient conditions. Windrow is the shape that mostly promotes drying in the summer and rewetting in winter. It is best to reduce pile size to facilitate drying in summer and increase pile size if material will be left in the field during winter. Drying times can be reduced by one-third if the material is cut and left drying during summer versus winter months.

Keywords: moisture content, drying rates, finite element analysis, harvest residues, Pacific Northwest

Starting in 2005, the Renewable Fuel Standard program requires increasing amounts of renewable fuel blended into transportation fuel sold or introduced into commerce in the United States. By 2022, 80 billion liters of advanced biofuel will be required. Out of this amount, 61 billion liters should be cellulosic biofuel (Energy Independence and Security Act of 2007), which may be derived from various sources, including woody biomass.

Forest harvest residues are widely available in the United States with estimates of more than 127 million cubic meters produced yearly (Smith et al. 2009). Despite a small demand from cogeneration plants, most of this material is burned in situ for site preparation and fire hazard reduction, mainly because of high production costs and a developing market (US Department of Energy 2011).

High moisture contents of woody biomass are a prohibitive factor in its application for bioenergy. Transportation costs can comprise up to 40% of the production cost (Zamora-Cristales et al. 2015); hence, it is important to improve efficiency in the context of moisture levels of transported materials. One notable inefficiency is that material with high moisture, potentially limits transportation capacity based on weight constraints, but not by volume. That is, a significant proportion of the payload is free and bound water. For example, reducing moisture content from 50 to 40% reduces transportation costs up to 18% due to the increased bulk volume (calculation based on transportation cost of 100$/hour and load weight capacity of 24 green metric tonnes). This inherent moisture is also a primary cause for losses in recoverable heat energy when used for power generation. When a cogeneration plant pays for delivered biomass depending on its moisture content, potential price premiums can be as high as 14% per dry ton for moisture content reduction from 50 to 30% wet basis (Sessions et al. 2013).

Moisture content of forest harvest residue has the potential for in situ drying with knowledge of ambient conditions. It responds to exposure to different environmental factors such as temperature, relative humidity, precipitation, and air flow (Hakkila 1989). Although ambient conditions cannot be controlled, other management factors can be altered in the context of environmental conditions to expedite the drying process. Wood is usually stacked to increase air flow and facilitate drying (Simpson and Wang 2003). In agriculture, hay is left to dry in windrows, and several studies have been performed to determine the effects of ambient conditions and conditioning on their drying (Thompson 1981, Smith et al. 1988, Savoie and Beauregard 1990). However, there is limited literature

Manuscript received August 22, 2016; accepted January 20, 2017; published online February 23, 2017.

Affiliations: *Francisca Belart (francisca.belart@oregonstate.edu), Department of Forest Engineering, Resources and Management, Oregon State University, Corvallis, OR. Ben Leshchinsky (ben.leshchinsky@oregonstate.edu), Oregon State University. John Sessions (john.sessions@oregonstate.edu), Oregon State University.*

Acknowledgments: *This research was funded by the Northwest Renewables Alliance (NARA). NARA is supported by the Agriculture and Food Research Initiative Competitive Grant 2011-68005-30416 from the US Department of Agriculture, National Institute of Food and Agriculture. We also want to thank MC Ranch, Lane Forest Products, OSU College Forests, Seneca Sustainable Energy LLC, Giustina Resources and Hancock Forest Management for giving us access to their forest land and operational assistance.*

Table 1. Site description for each unit.

Index	Site	Main species	Location	Elevation (m)	Average precipitation (mm)
CWH	Coast	Western hemlock	Depoe Bay, OR	122	1,779
VDL	Valley	Douglas fir	Corvallis, OR	235	1,029
VDH	Valley-East	Douglas fir	Dexter, OR	984	1,384
EPP	East	Ponderosa pine	La Grande, OR	1,158	457

describing the evaluation of the drying process for forest harvest residue, either experimentally or numerically.

Some studies have addressed the effect of storage time on forest harvest residue moisture content. Gautam et al. (2012) determined moisture content and fuel quality in the summer for piled residue of different ages (1, 2, 3 years old). Baxter (2009) determined changes in moisture for piled residue over 10 months using digital meters. Routa et al. (2015) determined residue moisture content changes over 35–85 weeks using constant weight monitoring. Afzal et al. (2010) determined piled residue internal moisture content with destructive methods in 3-month intervals over 1 year.

Gjerdrum and Salin (2009) built a drying model for poles using weather data and pole dimensions. Sikanen et al. (2012) developed biomass drying models for whole trees based on heuristics fitting and local weather in Finland. Kim (2012) developed drying models in Oregon for Douglas-fir (*Pseudotsuga menziesii* [Mirb.] Franco) and hybrid poplar (*Populus* sp.) small logs based on precipitation, evapotranspiration, and piece size using linear mixed-effects multiple regression models. These authors confirm the relationship between weather and drying rates in wood. However, none of them has focused on the use of physics to make moisture predictions or forest residue material.

Because real-time monitoring and instrumentation of residue piles are not practical on a large scale, modeling physical changes driving residue drying serves as a better means of evaluating drying of residue under field conditions. One potential approach toward evaluating coupled physical processes under transient conditions is through application of finite element analysis (FEA), which is used to solve sets of differential equations for a given continuum, boundary conditions, and constitutive properties, discretized through a finite mesh of interconnected elements and nodes. The FEA framework is frequently used to evaluate a variety of physical behaviors exposed to change, including structural analysis, thermodynamics, diffusion, electrical conduction, and drying behavior of wood under controlled conditions (Marchant 1976, Irudayaraj et al. 1992, Ferguson and Turner 1996, Kovács et al. 2010, Hozjan and Svensson 2011, ElGamal et al. 2013). The equations governing each element are solved through a system of equations that can give an approximation of the body behavior as a whole (Fagan 1992).

Ambient drying is a complex problem that involves various interdependent physics relationships, primarily including heat transfer, diffusion, and laminar flow (movement of air and moisture surrounding a continuum) but can also include solar radiation and, in some cases, turbulent flow (Curcio et al. 2008). Heat transfer occurs by three different mechanisms: radiation, convection, and conduction (Monteith and Unsworth 2008). In the model presented, convection and conduction are considered to describe heat transfer between surrounding air and the residue pile. Both depend on the temperature gradient between the pile and air, and area normal to the direction of heat flow. Convection will also depend on the convective heat transfer coefficient of the surrounding fluid (air/water) and conduction in both air and pile thermal conductivity (Welty et al. 2008). Diffusion describes the movement of species between media dependent on concentrations; in this case, the diffusion of moisture between the surrounding air and residue pile, which is most often described by Fick's law, demonstrating the relationship between the flux of diffusing species and the concentration gradient (Welty et al. 2008). Therefore, diffusion will depend on concentration gradient and diffusivity coefficients. For wood, diffusivity will depend on its moisture content because the water contained in cell lumens can escape at a different rate than water bound to the cell walls (Baronas et al. 2001). This water is chemically bonded, and it occurs when moisture content is below the fiber saturation point (Bowyer et al. 2003). Diffusion and heat transfer are also driven by fluid momentum transfer, which manifests in this case by the movement of moist air at the surface of the pile (boundary layer). The behavior of this layer depends on fluid properties (in this case air) such as viscosity, density, pressure, and velocity, and the momentum transfer associated with shear stresses (Monteith and Unsworth 2008). Often, the material properties are related and transient, typically varying with temperature and moisture content, necessitating a numerical analysis that can account for not only changing ambient conditions but also changing material properties with time, requirements satisfied with FEA.

FEA provides the flexibility of changing the drying season and duration, shape, size, location, porosity, moisture distribution within forest harvest residue piles, and other properties. These advantages cannot be achieved with the current methods, and this is the rationale for researching this methodology.

This project focuses on implementation of a FEA model that can aid in predicting moisture changes in piled forest harvest residues for given weather variables, informing opportunities to optimize drying of in-forest stored harvest residue. Data collected from a series of field experiments was used to build a series of baseline FEA models, enabling evaluation of drying sensitivity to various parameters. The results of these models provide further insight into pile drying behavior for given construction and ambient conditions, which can directly use data from a given weather station.

Methodology

Field Tests

To capture the primary regional climates and productive forest types of the Pacific Northwest, four monitoring units were set throughout the state of Oregon, located near Depoe Bay, Corvallis, Dexter, and La Grande and representing Coast western hemlock (*Tsuga heterophylla* [Raf.] Sarg.) (CWH) forest, low-elevation Douglas-fir forest (VDL), high-elevation Douglas-fir forest (VDH), and arid ponderosa pine (*Pinus ponderosa* Lawson and C. Lawson) (EPP) forest, respectively (Table 1). Each of these units contained three residue piles built specifically to monitor environmental variables and internal drying behavior of the residue. Residue piles were constructed within 1 month of tree harvest to maintain green moisture content as an initial condition, with the exception of the VDL

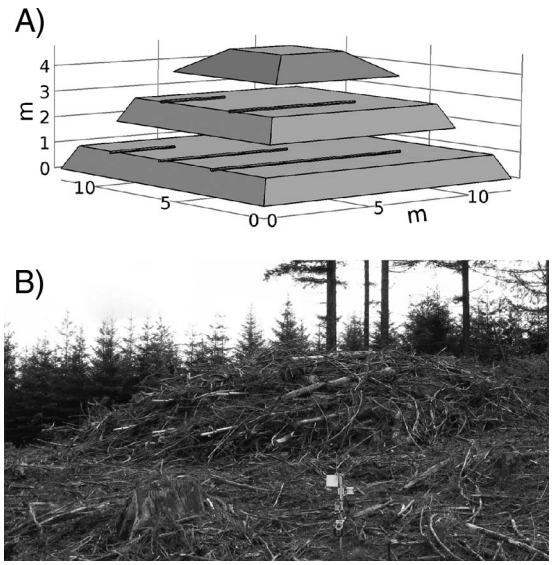

Figure 1. A. Schematic diagram of conduit placement in each pile B. Conduit placement on a pile in the field.

unit, which was constructed 2 months after harvest due to operation constraints. At pile construction, 30 wood samples were randomly cut (of all different diameters) from material that was going to be used to build each pile to determine the initial moisture content. For clarification purposes, these samples are named "S" samples though the document and represent a pile average moisture content.

Pile construction followed a consistent instrumentation framework. Construction of each pile occurred in three stages. First, a 12 × 12 m base pad of approximately 0.9 m in height was constructed with three evenly spaced (3 m) conduits of different lengths (9, 6, and 3 m) placed at the top of the constructed layer (Figure 1A) and equipped with 0.30-m-long mesh protectors at their ends (Figure 2A). After the conduit placement, another layer of harvest residue with a rectangular base of 9 × 9 m and height of 0.9 m was carefully placed on top, with subsequently placement of two more pieces of conduit of different lengths (6 and 3 m) on top. Finally, the pile of harvest residue was capped with a final residue layer, reaching a final height of 3.5 m. Once the conduit was located in the pile, a polyvinyl chloride (PVC) pipe (7.6 cm in diameter) of the same conduit lengths was used to introduce samples coupled with a temperature and relative humidity sensor in the pile (Figure 2B). These are referred to as "P" samples though the document, representing piece average moisture content. Each P sample was approximately 30 cm long and 3.8–4.3 cm in diameter, consisting of a branch or tree top taken from the same pile material. For protection, sensor cables ran through the PVC pipe, providing real-time data to HOBO Micro Station data loggers. Sensors were programmed to collect temperature and relative humidity readings every 3 minutes and report an hourly average. The mesh at the end of the pipe served as a protective measure while still enabling exposure to internal ambient conditions of the pile.

To comply with rules in Oregon, site preparation for reforestation needs to begin 1 year after harvest operations on a clearcut (Oregon Department of Forestry 2014), meaning that forest harvest residue would not remain in the field for longer than 12 months unless it does not constitute a fire hazard and does not interfere with the reforestation operation. For that reason, field data collection was limited to 1 year. Weather stations and pile sensors recorded data hourly for the 12-month monitoring period, whereas P samples were retrieved from the pile and weighed monthly with a scientific scale (0.5 g accuracy) to determine their green weight during storage (the monitoring schedule is shown in Table 2). After data collection was finished, these P samples were oven-dried to determine their dry weight and calculate the moisture content changes through the year. Weather stations installed next to each pile were monitoring precipitation, wind, temperature, and relative humidity. Finally, when piles were deconstructed, 10 more S samples of different diameters were randomly cut at four height levels of the piles (40 per pile) to determine final moisture content throughout the pile.

Finite Element Models

FEA was applied to evaluate the physical process of the instrumented, drying residue piles. Discrete evaluation of individual pieces of harvest residue, although a better representation of actual pile conditions, is difficult to model due to the uncertainty regarding the pile's porous matrix, distribution of material conditions, boundary conditions, and associated computational expense; therefore, continuum modeling of porous media was employed as a viable approach toward estimating pile behavior. Accounting for porosity within the FEA continuum enables reasonable evaluation of transient physical behavior for a pile matrix without the computational expense of modeling discrete branches or residue. The domain representing a given pile from field monitoring was designed as a half-ellipsoid with approximate 12-m width and 3-m height, surrounded by a box that was 10 m, 10 m, and 30 m in height, width, and depth, respectively (Figure 3). The box dimensions were selected from a sensitivity analysis that demonstrated negligible boundary effects on the given pile while maintaining computational efficiency. Assigned

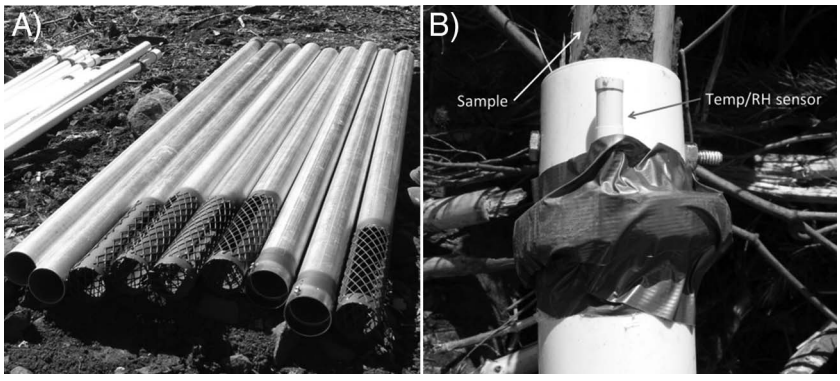

Figure 2. A. Electrical conduit with screen. B. Sample and temperature (Temp)/relative humidity (RH) sensor attached to PVC pipe.

Table 2. Schedule of testing sites and sampling.

	2014								2015											
Site	May	June	July	Aug.	Sept.	Oct.	Nov.	Dec.	Jan.	Feb.	Mar.	Apr.	May	June	July	Aug.	Sept.	Oct.	Nov.	Dec.
VDH	S,P	P	P	P	P	P	P	P	P	P	P	P	P,S							
VDL				S,P	P	P	P	P	P	P	P	P	P	P	P	P,S				
CWH						S,P	P	P	P	P	P	P	P	P	P	P	P	P,S		
EPP								S,P	P	P	P	P	P	P	P	P	P	P	P	P,S

P wood samples are permanently weighed with constant dimensions, and S samples cut at the beginning and end of each trial covering all ranges of diameters.

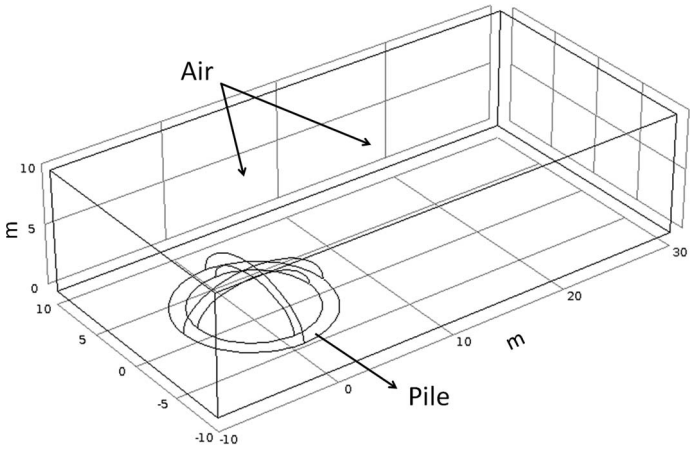

Figure 3. Diagram of pile and air domains in COMSOL.

to the given pile domain was an isotropic, homogeneous material representative of the porous matrix (properties are shown in Table 3), which applied properties presented in prior literature reports (e.g., TenWolde et al. 1988, Hardy 1996, Nield and Bejan 1998, Simpson and TenWolde 1999, Bowyer et al. 2003, Monteith and Unsworth 2008, Welty et al. 2008). Wood and air material properties were weighted proportional to porosity according to Nield and Bejan (1998) to obtain a better representation of the residue pile. The fluid properties of air were assigned to the surrounding box to represent ambient conditions.

To evaluate transient conditions within a given domain and material properties, meshing, initial conditions, and boundary conditions were assigned. A finer mesh was applied to the pile because a higher level of precision is needed in that domain and a coarser mesh was applied to the air; both domains were meshed using tetrahedral elements (0.46 m average element size). Because air is not a domain of interest, computational time can be saved by using a coarser mesh, especially around the edges. This analysis accuracy can be refined in areas of interest by increasing element density (reducing element size) where more precision is needed (Cook et al. 2001). Each physics module (heat transfer, laminar flow, convection, and diffusion) represents a set of governing differential equations that are coupled through various analytical approaches (Figure 4), notably, the Arrhenius equation, which determines diffusion through activation energy, the universal gas constant, and temperature (Welty et al. 2008).

Water is present in wood in two forms, free water and bound water. For this reason, the diffusion process occurs in two ways: free water may leave the cell lumens as water vapor and bound water is transferred cell by cell through their walls (Baronas et al. 2001). This water is chemically bonded to the cells, a process that requires more energy for the water to be released. According to Baronas et al. (2001), the diffusion coefficient depends on wood porosity, the bound water diffusion coefficient D_b, and the water vapor diffusion coefficient D_v.

The authors define the vapor diffusion as follows:

$$D_v = \frac{1.29 \times 10^{-13}\,(1 + 1.54u)\,p_s\,T_K^{1.5}}{(T_k + 254.18)} \cdot \frac{d\phi}{du} \qquad (1)$$

where u is moisture content, T_k is temperature in K (°), ϕ is relative humidity (%), and p_s is the saturated vapor pressure (Pa), defined as

$$p_s = 3{,}390e^{(-1.74+0.0759\,T_c-0.000424\,T_c^2+2.44\times10^{-6}\,T_c^3)} \qquad (2)$$

where T_c is temperature in ° C. The derivative of air relative humidity with respect to wood moisture content was calculated from sorption isotherms adapted by Simpson (1973) for wood after curve fitting and testing the Hailwood and Horrobin theory for hygroscopic materials. According to Baronas et al. (2001) the diffusion coefficient for bound water (D_b) can be defined with

Table 3. Material properties for the four sites.

		VDL, VDH, CWH		EPP	
Material property	Air	Wood (solid)	Pile (porous matrix)	Wood (solid)	Pile (porous matrix)
Porosity	1	0.67[1]	0.70[2]	0.72	0.70[2]
Bulk density (kg/m^3)	1	500[3]	150	420[3]	127
Thermal conductivity (W/m K)	0.025[4]	0.11[5]	0.05[6]	0.07[5]	0.04[6]
Heat capacity (J/kg K)	1,000[7]	1,250[3]	1,075[6]	1,250[3]	1,075[6]

Material properties for the western Oregon sites were assumed to be identical due to species composition.
[1] Based on 1,520 (kg/m^3) cell wall density (Bowyer et al. 2003).
[2] Data from Hardy (1996).
[3] Data from Simpson and TenWolde (1999).
[4] Data from Monteith and Unsworth (2008).
[5] Data from TenWolde et al. (1988) Wilkes equation.
[6] Data from Nield and Bejan (1998).
[7] Data from Welty et al. (2008).

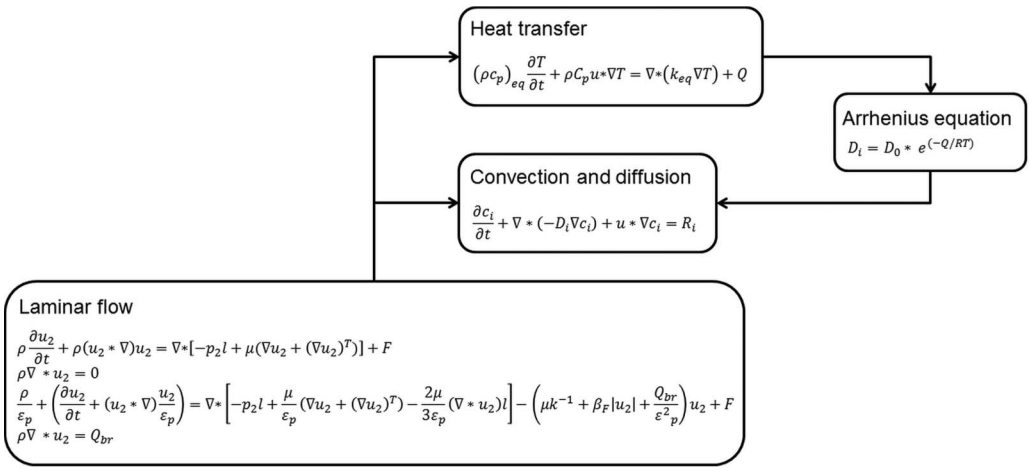

Figure 4. Diagram of physics modules and their association.

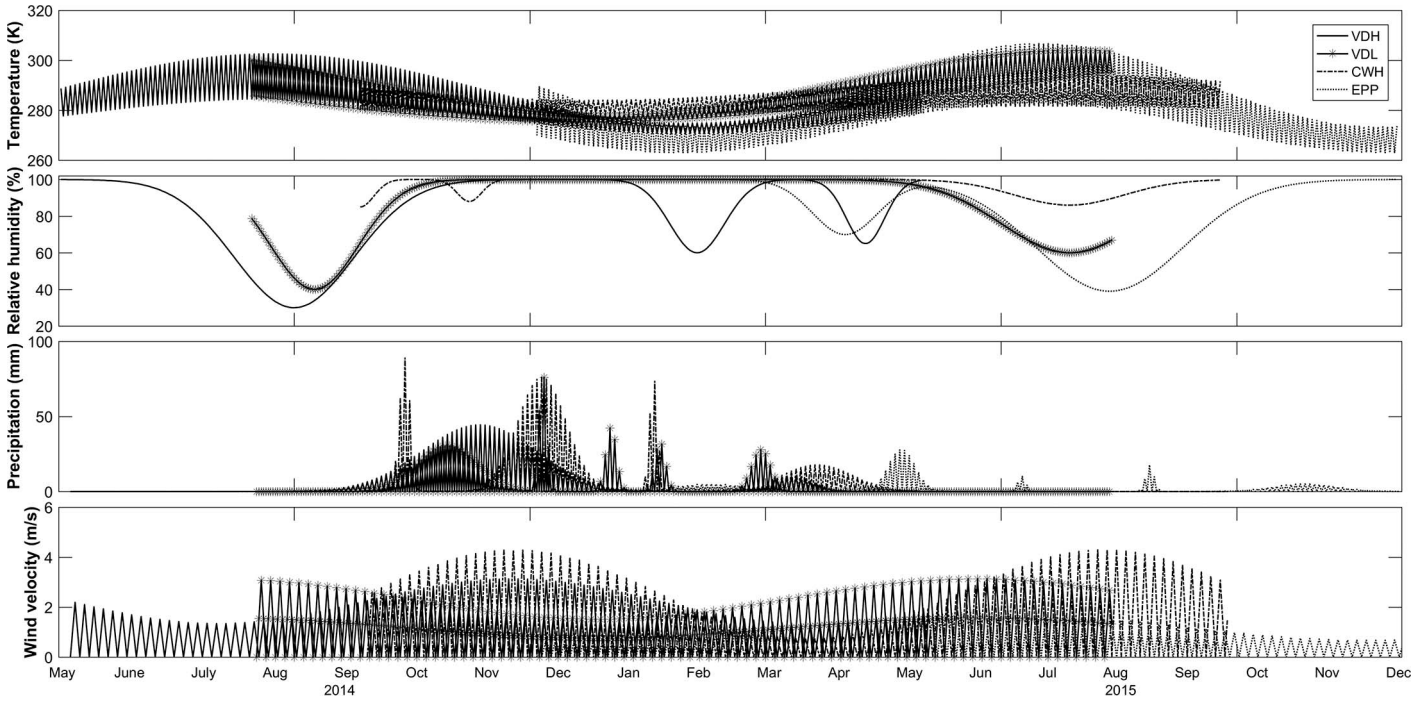

Figure 5. Functions for environmental variables on each site over their period of measurement.

the Arrhenius equation to determine the diffusion rate based on material activation energy, air temperature, and gas constant (8,314.3 kmol K). However, little information exists about relative diffusion rates for piles, which are a porous medium containing porous wood (small voids) and air (large voids); therefore, an effective diffusion rate was determined iteratively based on weighted, relative diffusion rates of wood and air based on wood diffusivity values reported by Nadler et al. (1985). In the specific case of the ponderosa pine site (EPP), the diffusion rate was set to zero during the winter freeze; it is assumed that there is no water movement during that period. That assumption was corroborated by the constant moisture content of the P samples located inside the pile during that time.

Input of Environmental Conditions

Weather stations measured environmental variables through a period of 1 year. To model these environmental factors, mathematical functions were created to approximate weather conditions, including wind, temperature, precipitation, and relative humidity for direct entry as boundary conditions for the FEA model. The time-dependent relationships for each site are presented in Figure 5.

These functions present an approximation of the data collected in the field starting in the month of May 2014 and ending in December 2015. Solar radiation was not considered in this model as boundary heating could occur, realizing a rise in external pile temperatures and marginal rise in internal pile temperatures. It was, however, omitted from this analysis for computational efficiency and a focus on the diffusion of moisture through diffusive processes greatly influenced by movement of air.

Boundary Conditions and Initial Conditions

Finite element models require initial conditions to define a representation of conditions before changes occur, specified as values

Table 4. Initial conditions for each site.

Site	MC_{wb} (%)	Pile and air temperature (K)	Wind velocity (m/s)
VDH	40	277.6	0
VDL	21	293.7	0
CWH	39	288.15	0
EPP	57	274.3	0

MC, moisture content; wb, wet basis.

Table 5. Model scaling parameters.

Site	VDH	VDL	CWH	EPP
Initial MC_{wb} (%)	34	21	39	54
Final moisture content	27	19	36	39
Diffusion rate (m^2/s)	2e−8	2e−8	1e−10	4e−8
Diffusion adjustment factor	20	20	4000	10

MC, moisture content; wb, wet basis.

on each domain. Boundary conditions are defined on boundaries of domains, representative of known values that govern the calculated differential equations within the enclosed domains. Initial conditions are based on experimental data and similar modeling techniques presented in literature reports (Curcio et al. 2008, Sandoval-Torres et al. 2011, ElGamal et al. 2013). The initial conditions for each test pile are presented in Table 4.

Specific boundary conditions are shown in Figure 6. Wind velocity was zero at ground level due to drag, at the inlet, there was a wind function (m/s) describing the wind fluctuations over time (shown in Figure 5), and in the outlet, the reference atmospheric pressure (1 atm) to solve for wind velocity. Temperature was set as a boundary condition in most walls to represent changes in temperature through the year. There was no heat transfer on the ground since soil temperature was not measured. Equilibrium moisture content was set as a boundary condition in inlet, top walls, and side walls so the wood in the pile would reach equilibrium, depending on changing temperature and relative humidity.

Solver

For this study, a commercially available FEA solver (COMSOL Multiphysics v5.1 with the heat transfer, laminar flow, and chemical reaction engineering modules) was used. After the input of appropriate properties and physics, a transient analysis was performed for given time increments, the maximum of which was 43,200 seconds (12 hours to capture both day and night conditions), subsequently analyzed in a postprocessing regime. To simulate the pile drying for 1 year (31,536,000 seconds), approximately 1½-20 hours of computing time was necessary on an Intel Core 2 PC (Windows 7 Enterprise, 3 GHz, 8 GB RAM).

Model Scaling

Because the residue pile consists of material of different sizes and species and the soil activity and water accumulation affecting the lowest portion of the pile is not modeled, the S samples taken at the beginning and end of the trial were used to scale the models at those two points in time. This adjustment was necessary to capture the behavior of the pile as an average, because the original model is based on, and validated with pieces of one particular diameter range. These adjustment factors were a function of initial and final pile moisture contents as well as diffusion rates; this because larger pieces of wood will dry at a slower rate than smaller pieces. However, future work could involve direct modeling of the pile as a whole to better capture the change in pile moisture conditions more objectively. The shape and the rest of the model parameters remained constant. Properties that were changed to scale the models are presented in Table 5. To distinguish these models from the originals, they will be referred to as "pile model."

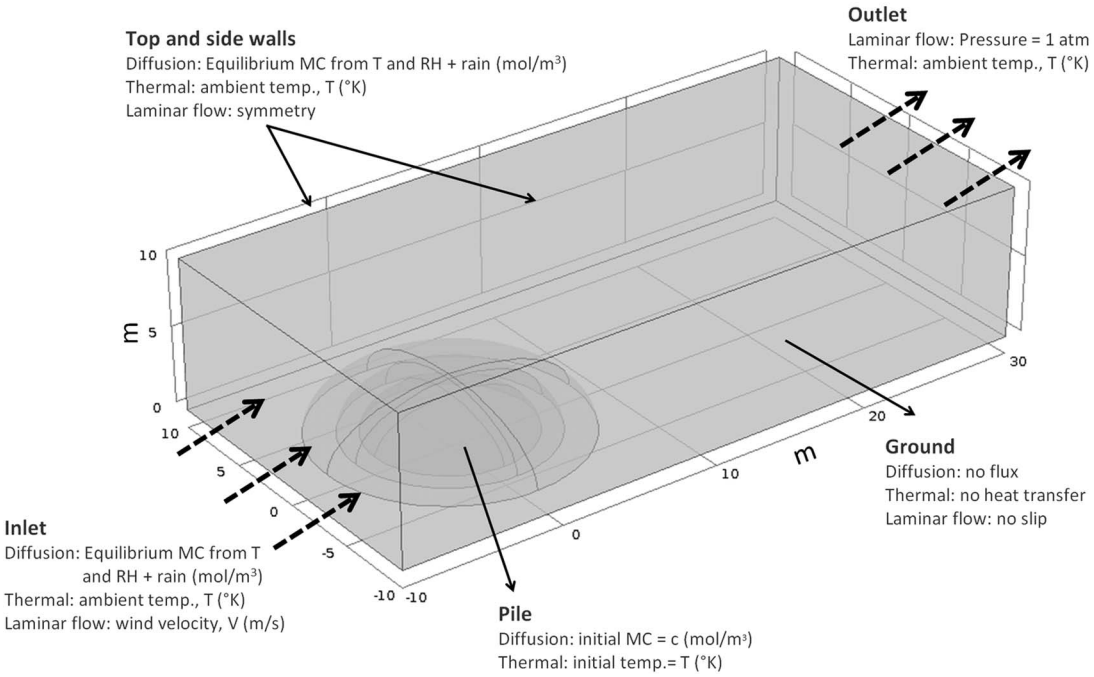

Figure 6. Boundary conditions for pile, ground, and surrounding air. MC, moisture content; RH, relative humidity; T, temperature.

Table 6. Model summary for sensitivity analysis.

Model	Site	Shape	Volume	Porosity	Start time (mo)
1	VDH	Half ellipsoid	Field (control)	0.7	0
2	VDH	Cone	Field (control)	0.7	0
3	VDH	Berm	Field (control)	0.7	0
4	VDH	Half ellipsoid	Half of field	0.7	0
5	VDH	Half ellipsoid	Double of field	0.7	0
6	VDH	Half ellipsoid	Field (control)	0.8	0
7	VDH	Half ellipsoid	Field (control)	0.9	0
8	VDH	Half ellipsoid	Field (control)	0.7	+3
9	VDH	Half ellipsoid	Field (control)	0.7	+6
10	VDL	Half ellipsoid	Field (control)	0.7	0
11	VDL	Cone	Field (control)	0.7	0
12	VDL	Berm	Field (control)	0.7	0
13	VDL	Half ellipsoid	Half of field	0.7	0
14	VDL	Half ellipsoid	Double of field	0.7	0
15	VDL	Half ellipsoid	Field (control)	0.8	0
16	VDL	Half ellipsoid	Field (control)	0.9	0
17	VDL	Half ellipsoid	Field (control)	0.7	+3
18	VDL	Half ellipsoid	Field (control)	0.7	+6
19	CWH	Half ellipsoid	Field (control)	0.7	0
20	CWH	Cone	Field (control)	0.7	0
21	CWH	Berm	Field (control)	0.7	0
22	CWH	Half ellipsoid	Half of field	0.7	0
23	CWH	Half ellipsoid	Double of field	0.7	0
24	CWH	Half ellipsoid	Field (control)	0.8	0
25	CWH	Half ellipsoid	Field (control)	0.9	0
26	CWH	Half ellipsoid	Field (control)	0.7	+3
27	CWH	Half ellipsoid	Field (control)	0.7	+6
28	EPP	Half ellipsoid	Field (control)	0.7	0
29	EPP	Cone	Field (control)	0.7	0
30	EPP	Berm	Field (control)	0.7	0
31	EPP	Half ellipsoid	Half of field	0.7	0
32	EPP	Half ellipsoid	Double of field	0.7	0
33	EPP	Half ellipsoid	Field (control)	0.8	0
34	EPP	Half ellipsoid	Field (control)	0.9	0
35	EPP	Half ellipsoid	Field (control)	0.7	+3
36	EPP	Half ellipsoid	Field (control)	0.7	+6

Sensitivity Analysis

After the models were scaled to represent whole-pile averages, the sensitivity analysis was performed. Many pile parameters can affect drying rates; in this study, pile shape, porosity, volume, and starting drying season were observed.

The first study presents the effects of shape, using a semi-ellipsoid as a baseline geometry representative of field conditions and both a cone and continuous berm shape of equivalent volumes for comparison (238 m^3). Besides changing the shape, the element size changed with the different geometries after the meshing process. Ranging from a minimum of 0.06 to 0.52 m maximum for the half-ellipsoid, 0.10 to 0.91 m for the cone, and 0.11 to 1.06 m for the berm.

Porosity (the volume of voids compared with the total volume of a porous matrix) was observed as a parameter that could affect drying rate. Porosity can vary for a given pile; therefore, three reasonable values within a 10% range were chosen for the second study: 70, 80, and 90%. In addition, half-ellipsoid piles of half (119 m^3) or double (476 m^3) the baseline volume (238 m^3) were evaluated for drying rates and defined as a third study. And finally, the effect of delaying the drying start time was evaluated. The baseline model starting time was delayed 3 and 6 months from the original starting date to assess its effect on drying. The starting month for VDH was May 2014, for VDL was August 2014, for CWH was October 2014, and for EPP was December 2014. The different studies that were implemented are summarized in Table 6.

Results

Model Comparisons

The monthly average moisture content obtained with the models was compared with the actual average moisture contents acquired in the field on each corresponding month (P samples). These P sample

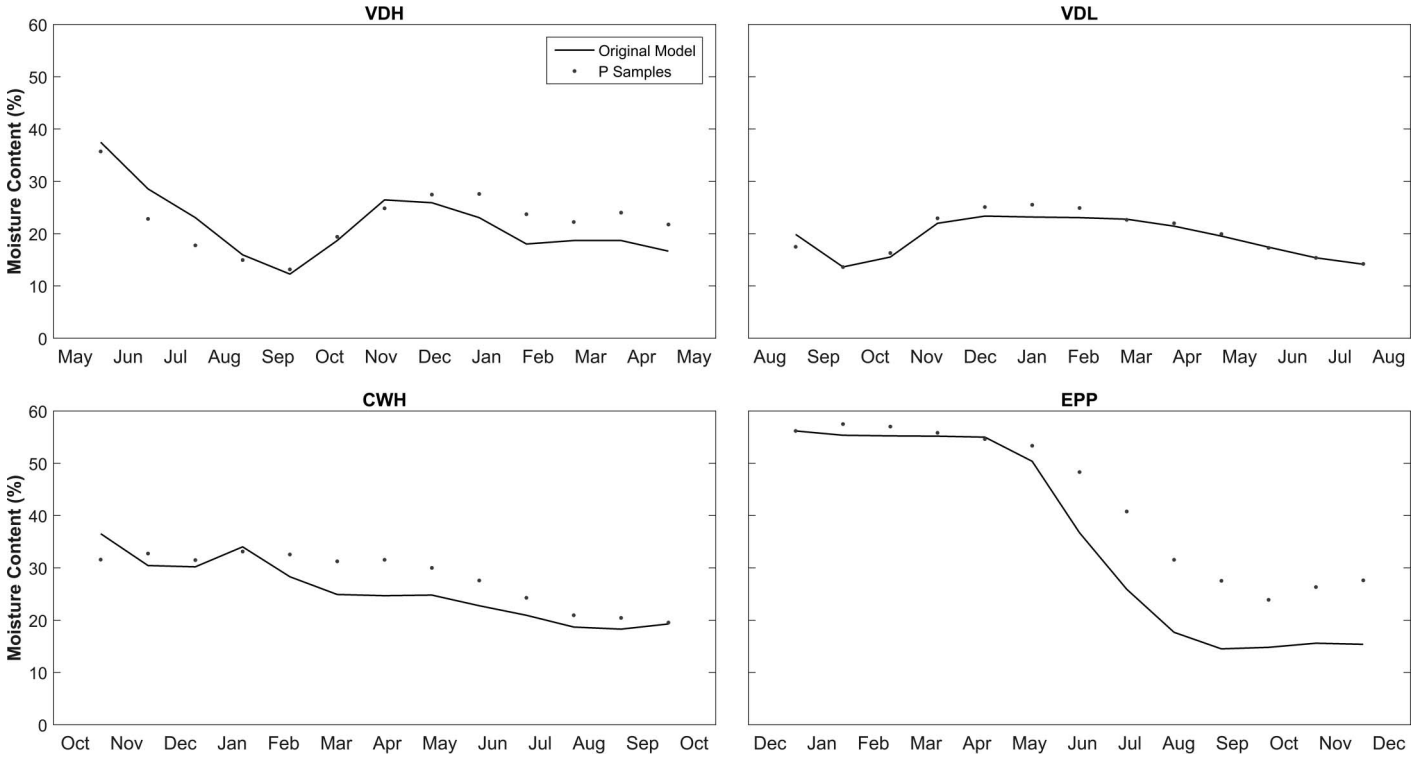

Figure 7. Modeled (original model) average moisture content (wet basis) versus field P samples.

Table 7. Model correlation and significance tests.

Site	Wilcoxon signed-rank test *P* value	Spearman's rho		Kendall's tau	
		Correlation	*P* value	Correlation	*P* value
VDH	0.4143	0.73	<2.2e−16	0.56	1.8e−6
VDL	0.1272	0.98	<2.2e−16	0.92	1.4e−7
CWH	0.0215	0.90	<2.2e−16	0.77	7.0e−5
EPP	0.0007	0.96	6.3e−3	0.87	6.7e−3

averages are used in the fitting tests as the time-dependent data are more robust and enable better evaluation of relative time-dependent drying and wetting. Both the modeled and sample averages follow a similar trend through the year (Figure 7). However, the greatest disparity can be seen at the EPP site.

Three statistical tests were performed to verify the agreement between the modeled moisture contents and data obtained in the field: a Wilcoxon signed-rank test, Kendall's tau and Spearman's rho correlation tests. At a 0.05 significance level, the modeled and field P sample average moisture content for the two Douglas-fir sites have an identical distribution (VDL and VDH Wilcoxon signed-rank tests, P value > 0.10). The other two site models (EPP and CWH) have a nonidentical distribution compared with field data. When correlation was tested, all sites present a statistically significant association between the model moisture content averages and field averages. The P values shown in Table 7 for Spearman's rho and Kendall's tau indicate that we can reject the null hypothesis that variables are uncorrelated at a 0.05 level. Spearman's rho indicates correlations >0.70 for all sites (Table 7). This parameter is more sensitive to differences compared with Kendall's tau because it compares the squared differences between pairs of data.

After the model was scaled to represent the overall pile moisture content, drying rates over time follow the same pattern as the base models. However, drying and rewetting occur at a slower rate. For that reason, the pile dries to a lesser extent over time, and moisture content is more stable throughout the year. The two points of comparison with S samples (pile initial − final moisture content) are represented in Figure 8.

Sensitivity Analysis

Shape

For the original model, on comparison of the 10-day moisture content averages of the control pile (half-ellipsoid, 0.7 porosity and volume 238 m^3) with the cone pile, differences in moisture content over time are very subtle with the exception of the EPP site, probably because of similar shape and length (6-m radius). However, the berm pile shows a marked difference (20-m length), especially in the drier and rainy months at the Douglas-fir sites. In the VDL site, the difference can be up to 12% higher moisture content in the winter and 7% lower in the summer (Figure 9).

When the model is scaled to pile averages (S samples), the effect of shape has the same trend as the original model (Figure 10), which is implicit owing to simple changing of the diffusion rate. For example, compared with the baseline shape, moisture content can be reduced by 3% during the dry season and rewet up to 5% moisture content during the rainy months in the valley Douglas-fir site.

Volume

Volume is the parameter that affects the drying rate of the piles the most. Material on a pile of the same shape and half the volume would have an average moisture content that was approximately 4–12% lower during the dry season and almost 9% higher during the wet months, depending on the site location and species (Figure 11). When the pile volume doubled, average

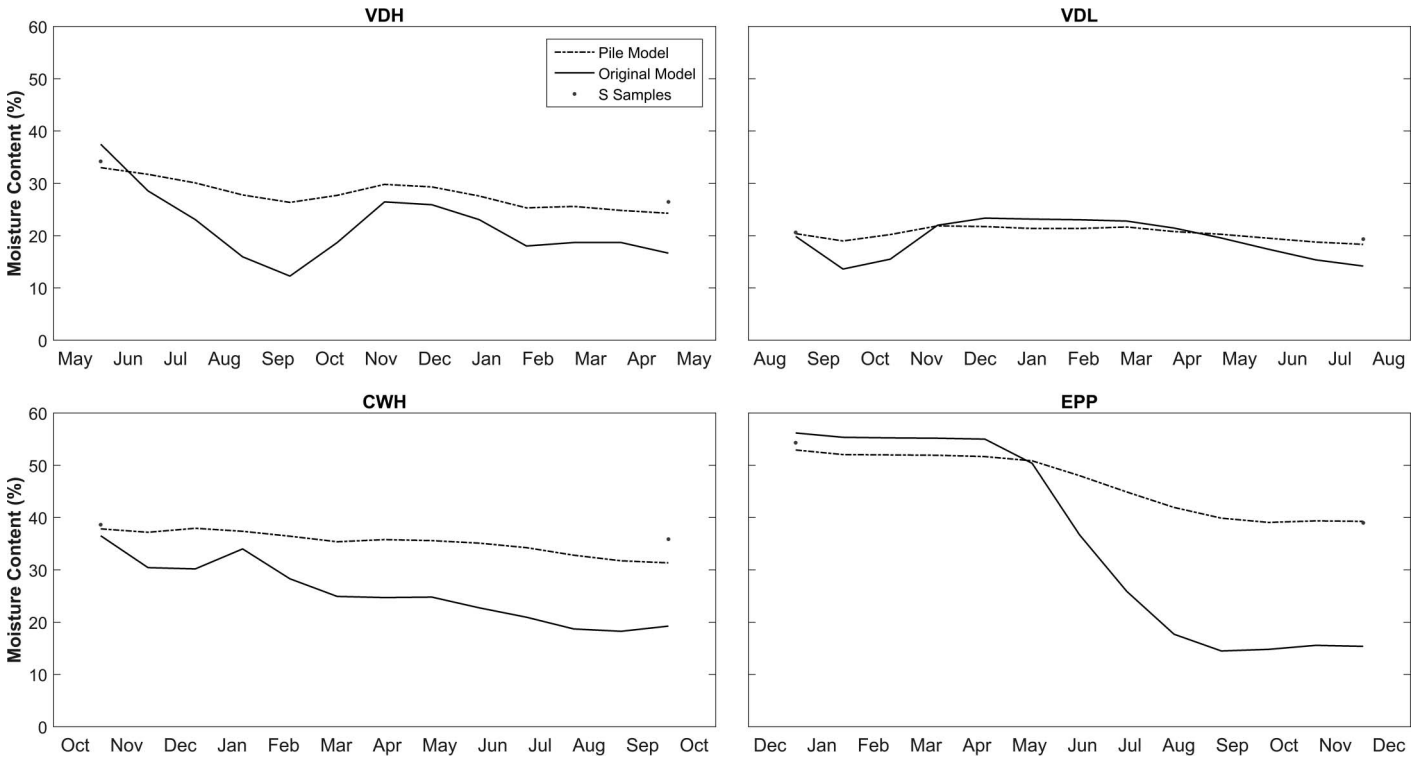

Figure 8. Modeled (pile-adjusted model) average moisture content (wet based) versus field S samples.

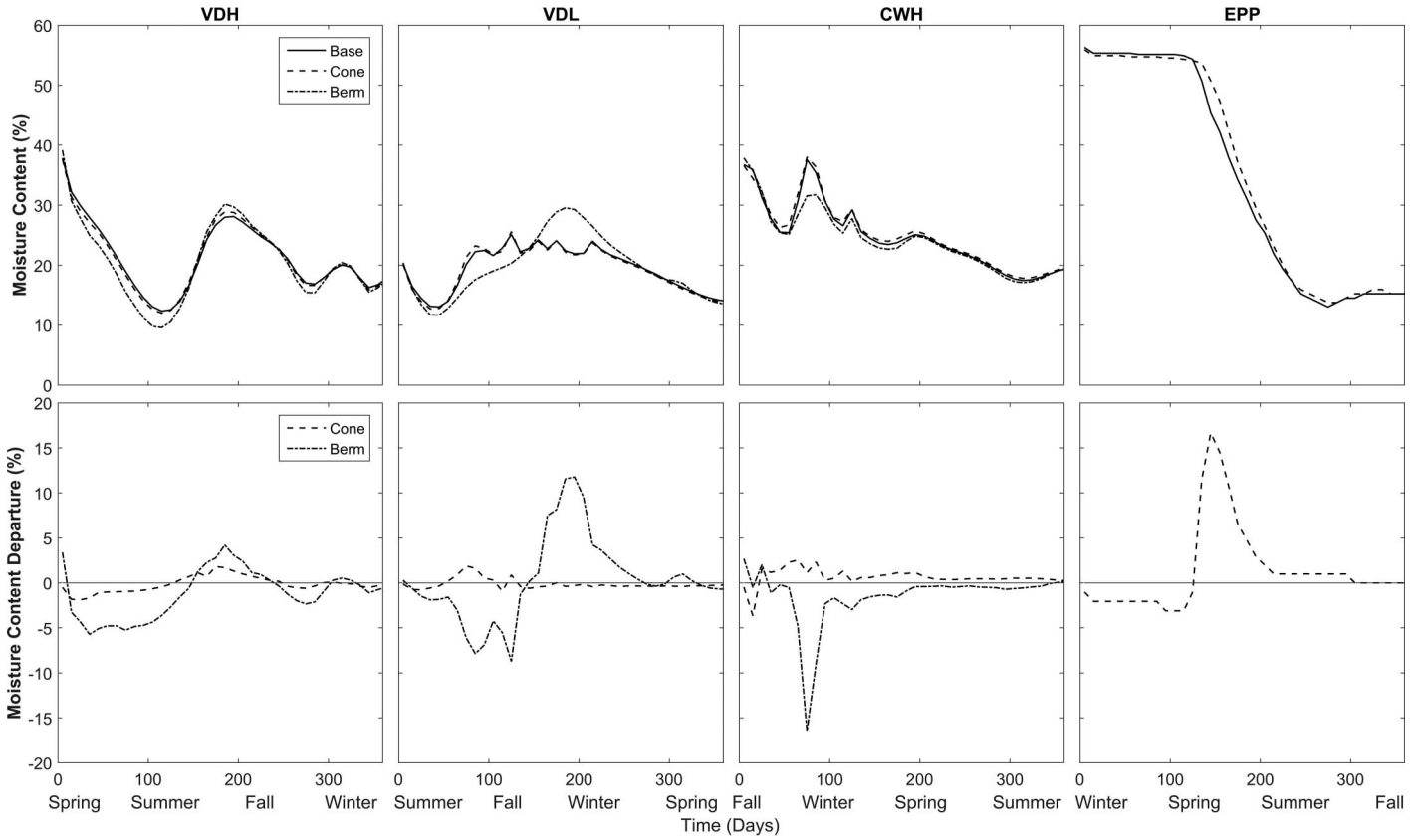

Figure 9. Shape effect on moisture content (wet basis) for each site, original model.

moisture content can be as much as 26% higher (EPP site) during dry months and, conversely, decrease during the rainy season compared with the baseline volume. The effect of pile volume is still the greatest within the sensitivity analysis when the models are scaled, but also realize diminished changes in moisture content (Figure 12).

Porosity

Porosity accentuates the effects of ambient conditions on pile behavior. With increasing porosity, the effects of drying and wetting become exaggerated within the residue pile (Figure 13). Average moisture content can be reduced by almost by 5% at any given time for the EPP site when porosity is increased by 0.2 (from 0.7 to 0.9) and increased by 19% during the rainy season when porosity is increased by 0.1 (from 0.7 to 0.8).

In the scaled model, the effect of porosity is marginal in the VDH and CWH sites and significantly smaller in the other two sites than in the original model. The greatest effects occur at the ponderosa pine site, where the pile rewets up to 9% more in a pile with a porosity of 0.8 than for the baseline (porosity of 0.7) during the spring rains (Figure 14).

Time

Even when the starting moisture content of the residue material that comprises a given pile remains constant, the drying rate changes depending on the starting point in which the material is stored in the forest. For example, in the VDH site, it takes 52 days for the material to reach an average moisture content less than 20% (wet basis) when drying starts in spring. If the same material is harvested and stored 3 months later, it would take only 8 days to reach that moisture content. Finally, if it was delayed another 3 months (6 months total), the residues would reach the same moisture content in 73 days. As expected, when drying starts during the dry and warm months, the residue will approach lower moisture contents faster, reaching equilibrium with environmental conditions more expediently (Figure 15).

Similar to other parameters, the scaled model has a smaller impact with time changes. For the VDL site, the effect is marginal. However, for the EPP site, it takes 196 days for the average moisture content to reach levels less than 43% (wet basis) if drying starts in winter, 115 days in spring, and only 33 days in summer (Figure 16).

Discussion

The series of models presented here offered reasonable agreement with field drying rates, confirmed by results of statistical tests compared with field data (Table 7). This sets a framework to define and compare different means of in situ residue drying for specific ambient conditions. Although it is difficult to represent all potential conditions, the impact of parameters critical to drying may be evaluated. For all sites, residue piles dry fast during the first months, finding particular dependence on the time of harvest, often reaching a minimum in September–October. The ponderosa pine site (EPP) has almost no drying during the first months, because there is no diffusion during the winter deep freeze. Rain, along with lower temperatures and higher relative humidity, allows the material to remoisten during the wet rainy season.

After the model was scaled with S samples, results showed the same trends as the base original models, with lower drying rates. Material of larger sizes dries at a slower rate. For these models, there is little drying in either valley Douglas-fir or coast western hemlock

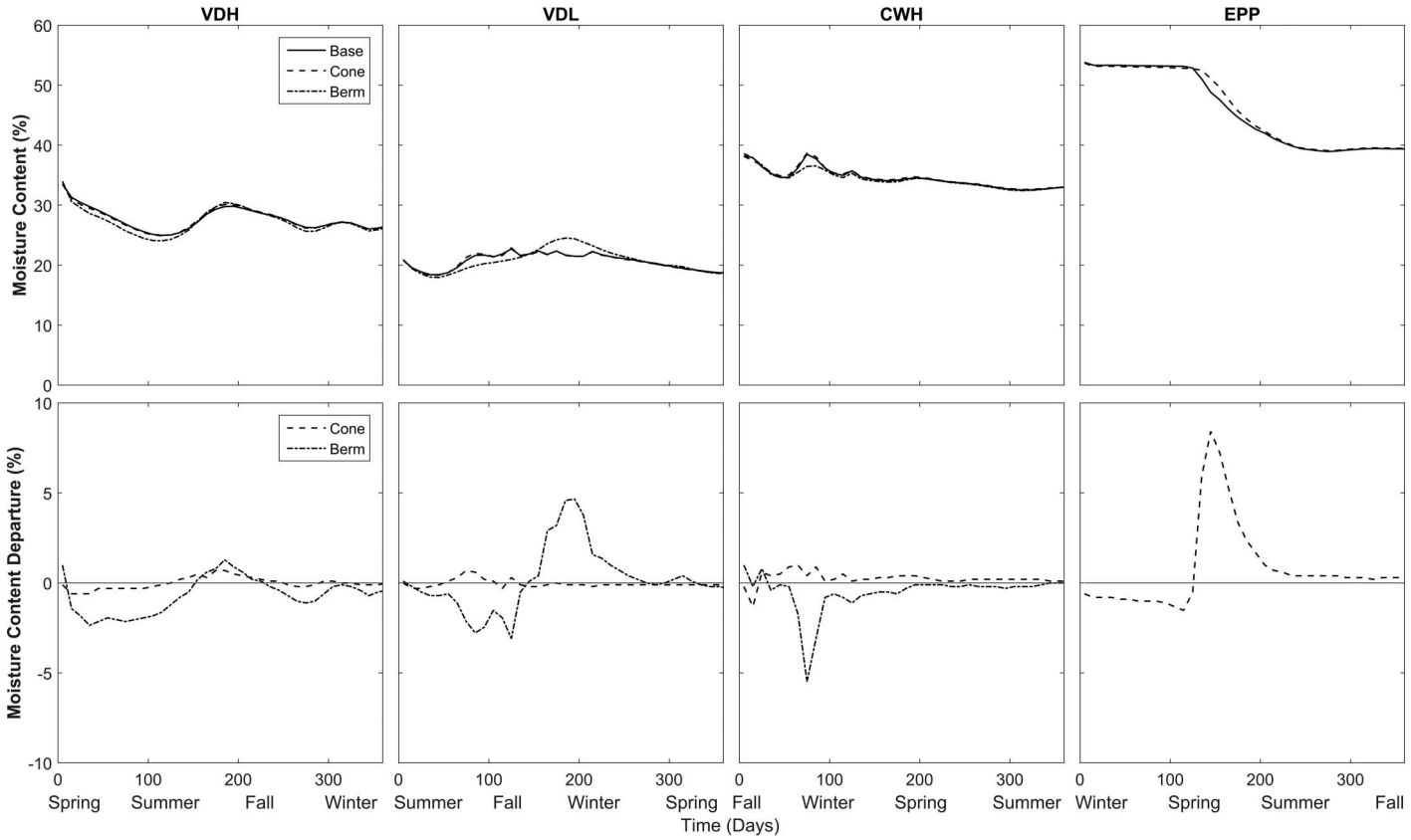

Figure 10. Shape effect on moisture content (wet basis) for each site, pile model.

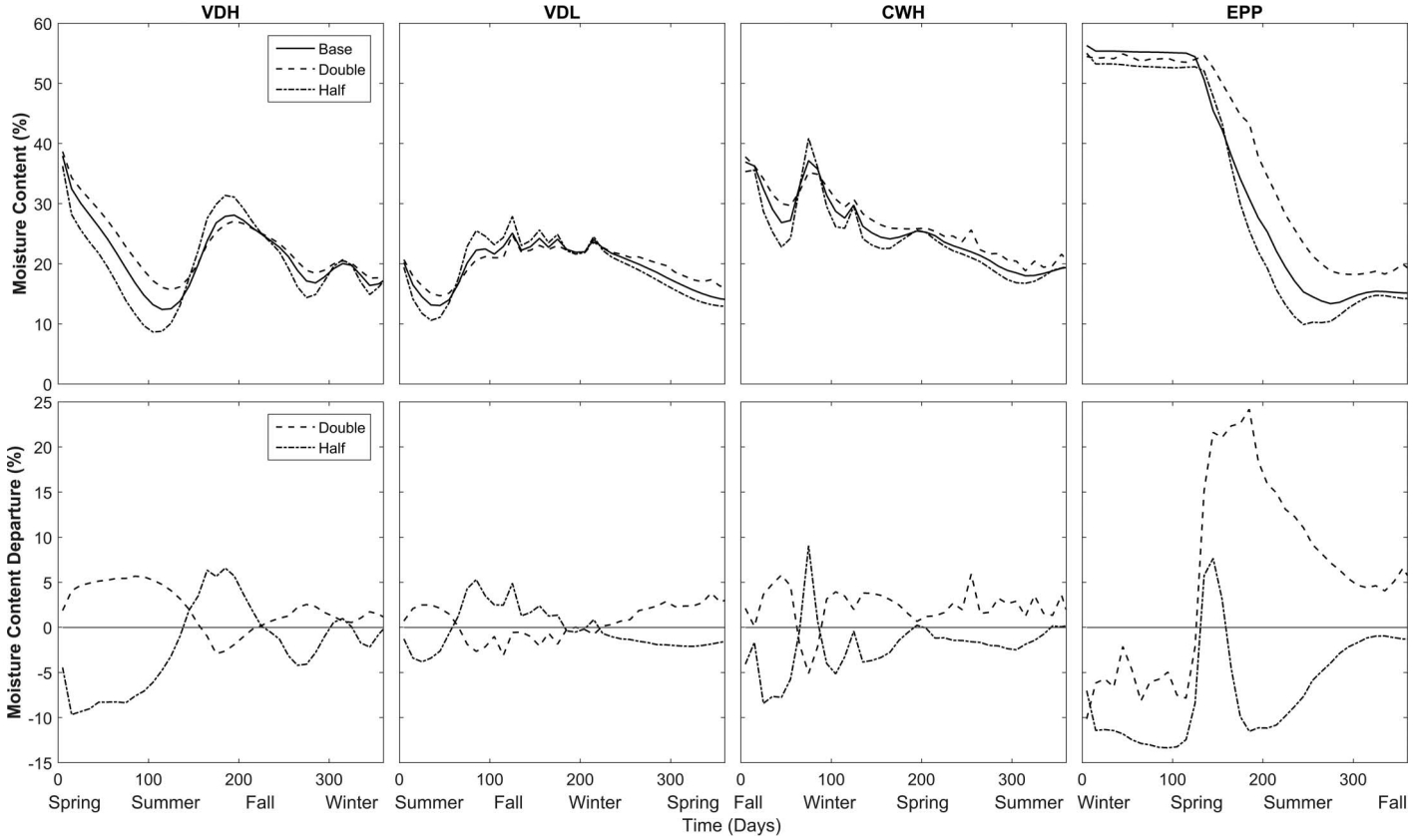

Figure 11. Effect of pile volume on moisture content for each site, original model.

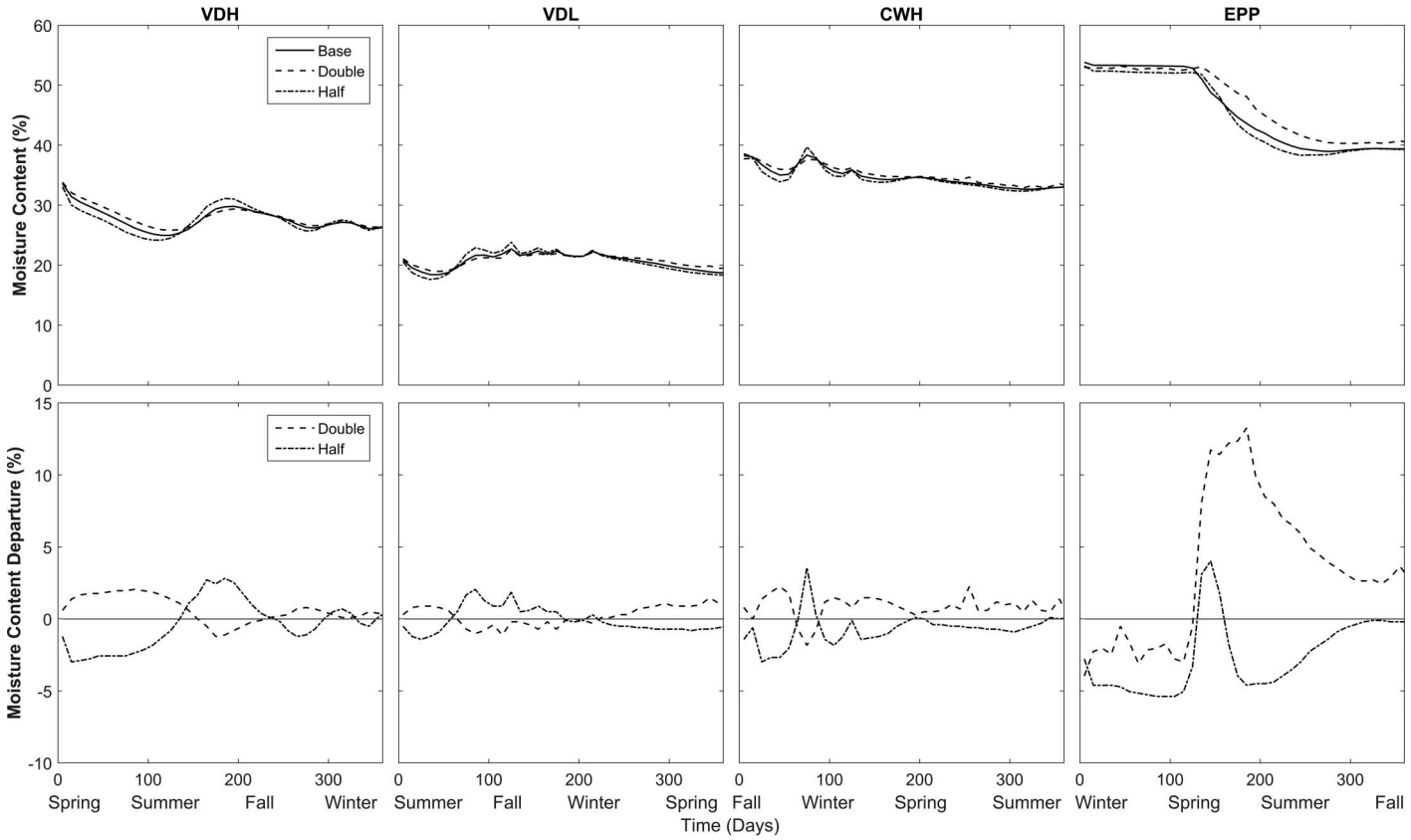

Figure 12. Effect of pile volume on moisture content for each site, pile model.

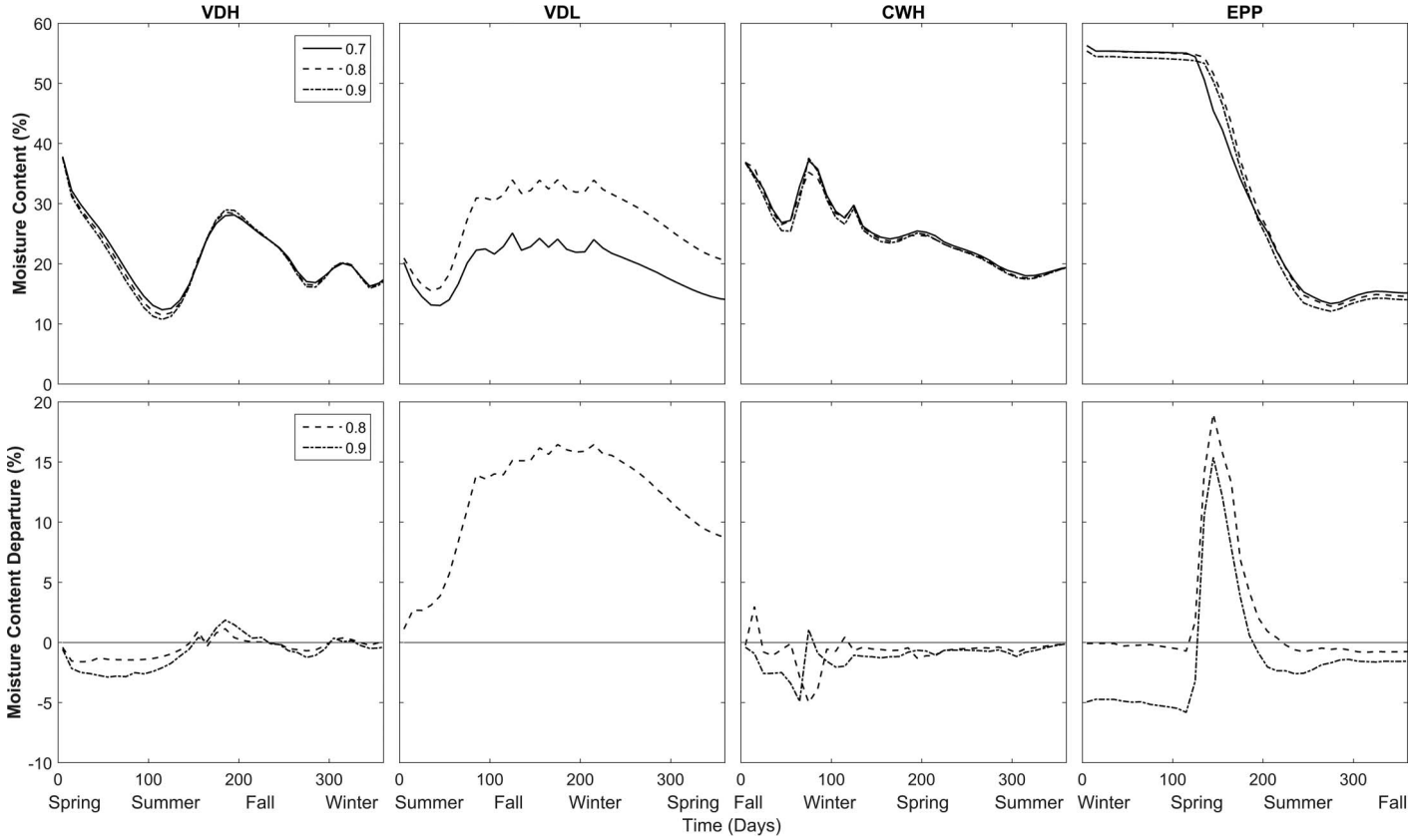

Figure 13. Effect of pile porosity on moisture content for each site, original model.

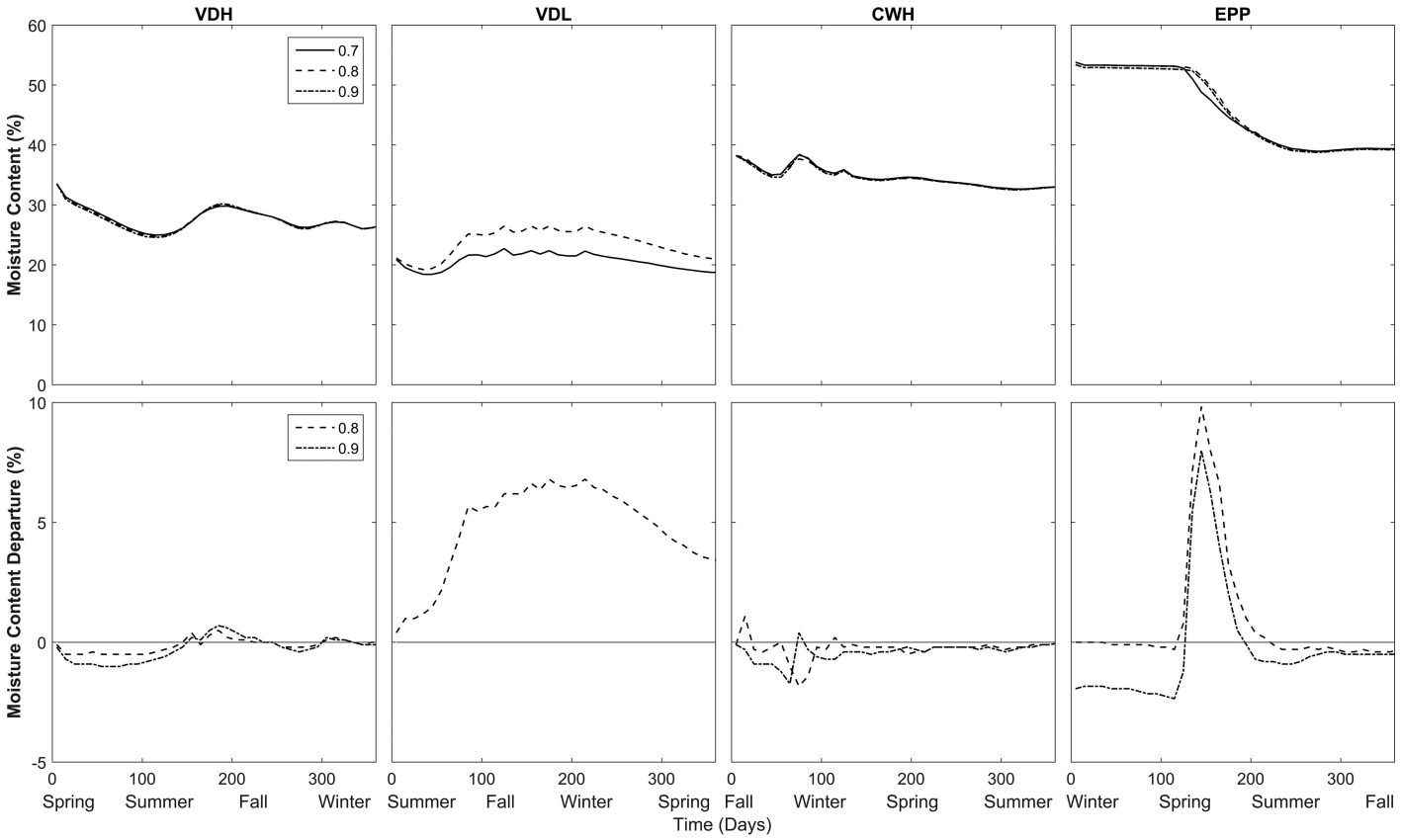

Figure 14. Effect of pile porosity on moisture content for each site, pile model.

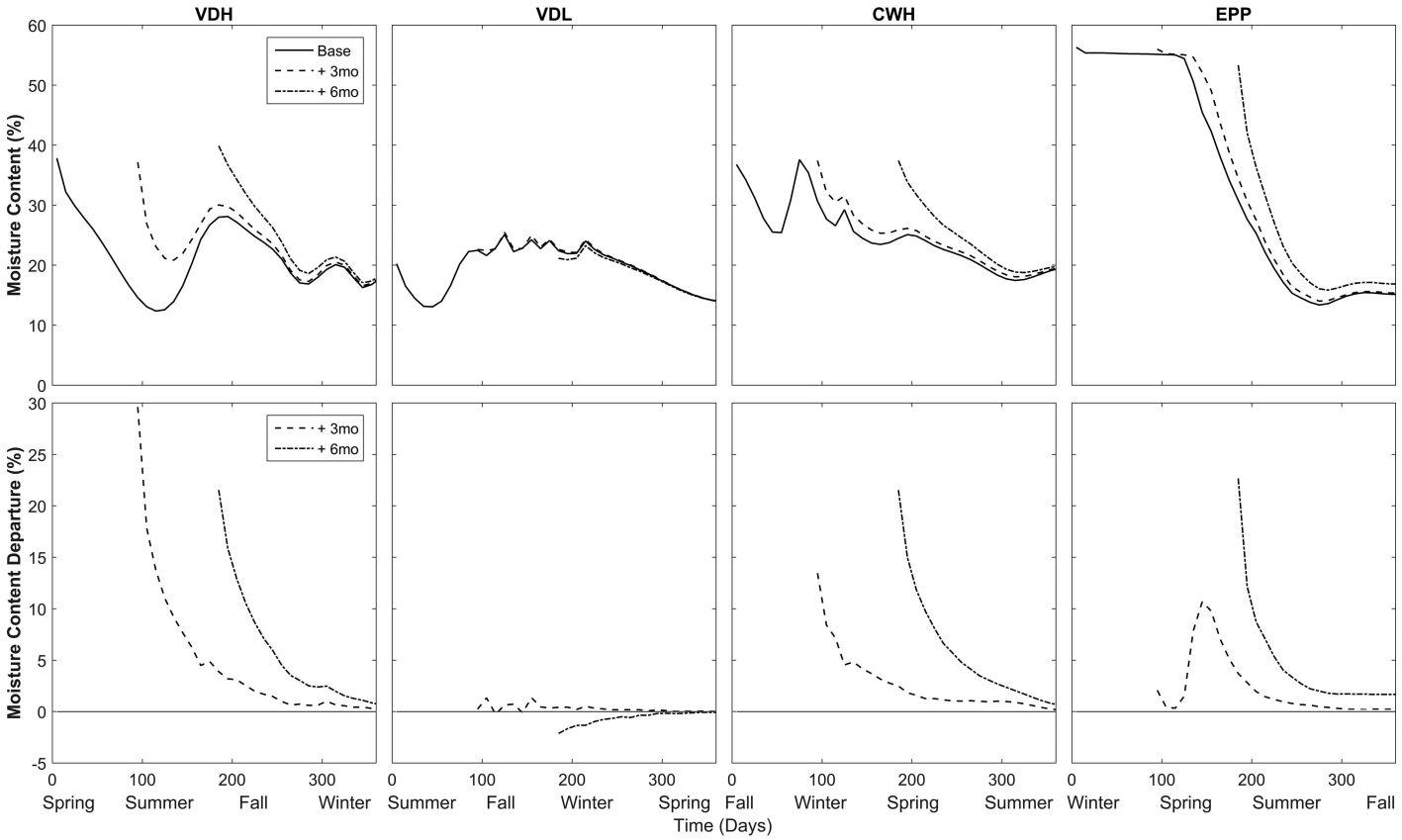

Figure 15. Effect of drying time on moisture content for each site, original model.

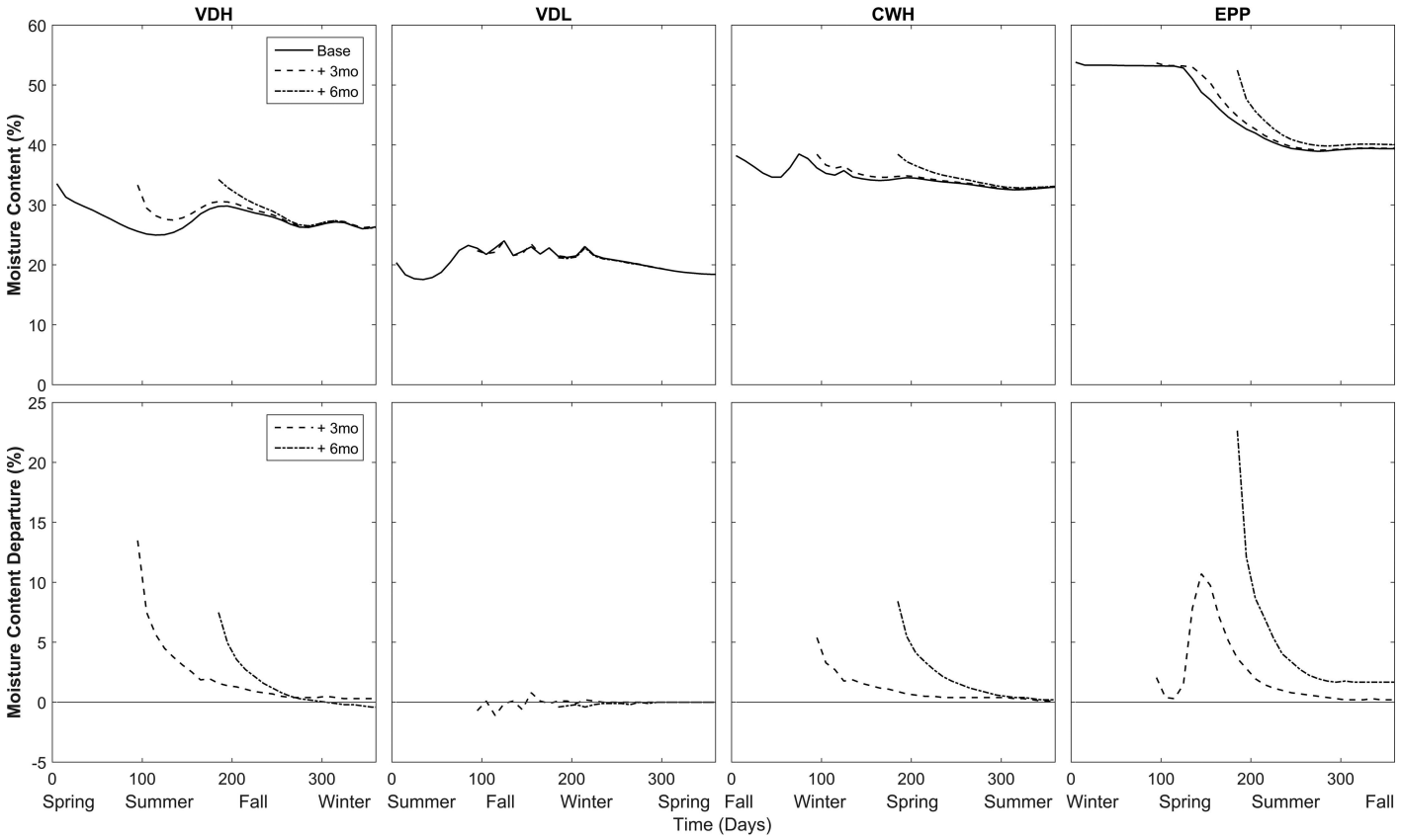

Figure 16. Effect of drying time on moisture content for each site, pile model.

after 1 year of field storage. Some possible reasons are that the Douglas-fir began with dry material, probably muting the observed drying effects. The CWH unit was continuously under the effect of marine moist air, which could be the explanation for stability of the material's moisture content. The greatest drop in moisture content is observed in the EPP unit; this could be caused by the material being very wet at the start of the trial and the likely lag of freezing preventing diffusion of moisture, particularly underneath a layer of snow.

As expected, berm or windrow geometry works best to expedite the drying process because of the large relative surface area and exposure to ambient conditions and convection. This shape has 60% larger surface area directly exposed to wind, which is probably the main cause for the differences. Residue moisture content is reduced between 2 and 5% compared with that of a half-ellipsoid of the same volume during the dry season. However, the same advantageous conditions for drying may also expedite rewetting in the winter, probably because more surface area is directly exposed to rain. The cone shape behaves similarly to the half-ellipsoid for all sites probably owing to a generally similar shape in relative surface area.

Volume is the parameter that most affects drying. When the pile volume is halved, moisture content can be reduced by 2–5% during the dry months and increased by 3–4% during the wet season in comparison to baseline volume. When the volume is doubled, moisture content can increase from 1 to 13%, depending on the site. These changes are probably driven by the same principles that affect the different pile shapes. A pile with smaller volume allows more airflow through the interior of the pile, permitting more efficient drying. At the same time, there is less coverage from the rain, allowing more moisture to reach the material inside the pile. A larger pile, has the opposite effect: more material is protected from wind and rain.

Porosity is a pile property that is difficult to change in a practical sense but may have impacts on the rates of drying or wetting for given ambient conditions. Increasing the porosity has a greater effect on sites such as VDL and EPP, where more voids may increase sensitivity to weather conditions for the baseline model presented (porosity of 0.7).

The time of harvest has notable effects on residue drying times because the gradient in moisture or temperature for a given time of year may expedite or slow drying. For example, in the case of the ponderosa pine site (EPP), it can take one-sixth of the time it takes for the residue to reach 43% moisture content when drying starts in summer versus winter. During summer, higher temperature and lower relative humidity reduce the wood equilibrium moisture content, and there is little or no rewetting of the material.

Conclusions

Finite element models were developed for four sites representing the main climatic regions in Oregon and their respective commercialized forest species. These models are able to sufficiently capture forest residue drying rates within the pile with weather data input such as precipitation, wind, ambient temperature, and relative humidity. These diffusion rates, however, are dependent on the measured piece size, making scaling an important consideration for evaluating the whole pile's drying behavior. For this reason, scaling factors were necessary to better represent the entire pile's drying behavior. Future work could better capture the inhomogeneous nature of the pile's piece sizes, corresponding diffusion rates, and

packing density in a more objective manner. FEA may provide a means of performing this task. Our conclusions include the following:

- Piled residue moisture content responds to the environmental conditions greatly. The selection of pile shape or size can be beneficial or detrimental to the rate of drying, depending on ambient conditions. Future work could better capture the effects of the preferential, non-Darcy flow of precipitation through the voids of a pile, given varying pile shapes, sizes, and piece size distributions.
- A berm (windrow) presents the best option for expedient drying because of its large surface area. Drying is the fastest in this shape during dry summer months; however, the pile also rewets the fastest during wet, winter months.
- It is best to reduce pile volume if storage will occur through summer and increase size if it will occur through winter. The reason behind this is the same as for the shape: a smaller pile will have more airflow, but it will also become wetter in the rainy season than a larger pile.
- Significant reduction in drying times can be achieved if the material is cut and left to dry during the dry, warm summer months. This reduction can be up to one-third of the time versus starting the process in the winter.
- This methodology is a tool that has the flexibility to be able to change parameters and conditions in which the harvest residues are stored. For that reason, it opens several possibilities for future research.

The models presented here were made with local data, and inferences are generally specific to these locations. However, the main concepts and sensitivity of pile drying parameters still present a general understanding for drying conditions in many different climates. As part of future work, the effect of aspect and slope on drying rates will be assessed. In addition, changing pile porosity with depth will be implemented to produce a refined model. It is anticipated that this change could result in a better model fit with the field sample averages.

Literature Cited

AFZAL, M., A. BEDANE, S. SOKHANSANJ, AND W. MAHMOOD. 2010. Storage of comminuted forest biomass and uncomminuted forest biomass and its effect on fuel quality. *BioResources* 5(1):55–69. https://www.ncsu.edu/bioresources/BioRes_05_1.html#Afzal_Storage_Comminuted.

BARONAS, R., F. IVANUSKAS, I. JUODEIKIENE, AND A. KAJALAVICIUS. 2001. Modelling of moisture movement in wood during outdoor storage. *Nonlinear Anal. Model. Control* 6(2):3–14. Available online at http://www.mii.lt/na/issues/NA_0602/NA06201.pdf.

BAXTER, G. 2009. *Assessing moisture content of piled woody debris: Implications for burning.* FPInnovations FERIC, Wildland Fire Operations Group. 15 p.

BOWYER, J., R. SHMULSKY, AND J. HAYGREEN. 2003. *Forest products and wood science: An introduction*, 4th ed. Blackwell Publishing, Oxford, UK. 554 p.

COOK, R., D. MALKUS, M. PLESHA, AND R. WITT. 2001. *Concepts and applications of finite element analysis*, 4th ed. John Wiley & Sons, New York. 719 p.

CURCIO, S., M. AVERSA, V. CALABRÒ, AND G. IORIO. 2008. Simulation of food drying: FEM analysis and experimental validation. *J. Food Eng.* 87(4):541–553. doi:10.1016/j.jfoodeng.2008.01.016.

ELGAMAL, R., F. RONSSE, AND J.G. PIETERS. 2013. Modeling deep-bed grain drying using COMSOL Multiphysics. In *COMSOL conference proc.*, Rotterdam, The Netherlands. Oct. 23–25, 2 p. Available online at https://www.comsol.com/paper/modeling-deep-bed-grain-drying-using-comsol-multiphysics-15371.

FAGAN, M.J. 1992. *Finite element analysis, theory and practice.* Longman Scientific & Technical, Essex, UK. 315 p.

FERGUSON, W.J., AND I.W. TURNER. 1996. A control volume finite element numerical simulation of the drying of spruce. *J. Comp. Phys.* 125(1):59–70. doi:10.1006/jcph.1996.0079.

GAUTAM, S., R. PULKKI, CH. SHAHI, AND M. LEITCH. 2012. Fuel quality changes in full tree logging residue during storage in roadside slash piles in Northwestern Ontario. *Biomass Bioenergy* 42:43–50. doi:10.1016/j.biombioe.2012.03.015.

GJERDRUM, P., AND J.-G. SALIN. 2009. Open air drying of Scots pine transmission poles prior to creosote treatment. P. 95–102 in *Proc. "Wood science and engineering in the third millennium."* Brasov, Romania.

HAKKILA, P. 1989. *Utilization of residual forest biomass.* Springer-Verlag, New York. 568 p.

HARDY, C. 1996. *Guidelines for estimating volume, biomass, and smoke production for piled slash.* USDA Forest Service, Gen. Tech. Rep. PNW-GTR-364. Pacific Northwest Station, Portland, OR. 17 p. https://www.fs.fed.us/pnw/publications/pnw_gtr364/.

HOZJAN, T., AND S. SVENSSON. 2011. Theoretical analysis of moisture transport in wood as an open porous hygroscopic material. *Holzforschung* 65(1):97–102. doi:10.1515/hf.2010.122.

IRUDAYARAJ, J., K. HAGHIGHI, AND R. STROSHINE. 1992. Finite element analysis of drying with application to cereal grains. *J. Agric. Eng. Res.* 53:209–229. doi:10.1016/0021-8634(92)80084-6.

KIM, D.-W. 2012. *Modeling air-drying of Douglas-fir and hybrid poplar biomass in Oregon.* MSc thesis. Oregon State Univ., Corvallis, OR. 56 p.

KOVÁCS, A., E. LAKATOS, G. MILICS, AND M. NEMÉNYI. 2010. Finite element modeling of coupled heat and mass transfer of a single maize kernel based on water potential using COMSOL Multiphysics simulation. In *COMSOL conference Proc.*, Paris, France. Nov. 17–19, 5 p. Available online at https://www.comsol.com/paper/finite-element-modeling-of-coupled-heat-and-mass-transfer-of-a-single-maize-kern-8053.

MARCHANT, J. 1976. The prediction of airflows in crop drying systems by the finite element method. *J. Agric. Eng. Res.* 21(4):417–429. doi:10.1016/0021-8634(76)90061-5.

MONTEITH, J., AND M. UNSWORTH. 2008. *Principles of environmental physics*, 3rd ed. Academic Press, San Diego, CA. 418 p.

NADLER, K., E. CHOONG, AND D. WETZEL. 1985. Mathematical modeling of the diffusion of water in wood during drying. *Wood Fiber Sci.* 17(3):404–423. https://wfs.swst.org/index.php/wfs/article/view/514.

NIELD, D.A., AND A. BEJAN. 1998. *Convection in porous media*, 2nd ed. Springer, New York. 546 p.

OREGON DEPARTMENT OF FORESTRY. 2014. *Forest Practice Administrative Rules and Forest Practices Act.* Chap. 629. Forest Practices Administration, Salem. OR. 94 p.

ROUTA, J., M. KOLSTRÖM, J. RUOTSALAINEN, AND L. SIKANEN. 2015. Precision measurement of forest harvest residue moisture change and dry matter losses by constant weight monitoring. *Int. J. For. Eng.* 26(1):71–83. doi:10.1080/14942119.2015.1012900.

SANDOVAL-TORRES, S., W. JOMAA, J.-P. PUIGGALI, AND S. AVRAMIDIS. 2011. Multiphysics modeling of vacuum drying of wood. *Appl. Math. Model.* 35(10):5006–5016. doi:10.1016/j.apm.2011.04.011.

SAVOIE, P., AND S. BEAUREGARD. 1990. Predicting the effects of hay swath manipulation on field drying. *Trans. ASAE.* 33(6):1790–1794. doi:10.13031/2013.31541.

SESSIONS, J., K. TUERS, K. BOSTON, R. ZAMORA, AND R. ANDERSON. 2013. Pricing forest biomass for power generation. *West. J. Appl. For.* 28(2):51–56. doi:10.5849/wjaf.12-012.

SIKANEN, L., D. RÖSER, P. ANTTILA, AND R. PRINZ. 2012. *Forecasting*

algorithm for natural drying of energy wood in forest storages. Forest Energy Observer Study Rep. 27. Finnish Forest Research Institute, Helsinki, Finland. 7 p.

SIMPSON, W.T. 1973. Predicting equilibrium moisture content of wood by mathematical models. *Wood Fiber* 5(1):41–49. https://wfs.swst.org/index.php/wfs/article/view/740.

SIMPSON, W., AND A. TENWOLDE. 1999. Physical properties and moisture relations of wood. P. 3.1–3.24 in *Wood handbook: Wood as an engineering material.* USDA Forest Service, Gen. Tech. Rep. FPL-GTR-113, Forest Products Laboratory, Madison, WI. https://www.treesearch.fs.fed.us/pubs/5734.

SIMPSON, W.T., AND X. WANG. 2003. *Estimating air drying times of small-diameter ponderosa pine and Douglas-fir logs.* USDA Forest Service, Res. Pap. FPL-613, Forest Products Laboratory, Madison, WI. 14 p. https://www.treesearch.fs.fed.us/pubs/6350.

SMITH, E., E. DUNCAN, M. MCGECHAN, AND D. HAUGHEY. 1988. A model for the field drying of grass in windrows. *J. Agric. Eng. Res.* 41(4):251–274. doi:10.1016/0021-8634(88)90212-0.

SMITH, W., P. MILES, CH. PERRY, AND S. PUGH. 2009. *Forest resources of the United States, 2007.* USDA Forest Service, Gen. Tech. Rep. WO-78, Washington, DC. 336 p. https://www.treesearch.fs.fed.us/pubs/17334.

TENWOLDE, A., J.D. MCNATT, AND L. KRAHN. 1988. *Thermal properties of wood and wood panel products for use in buildings.* Rep. DOE/USDA-21697/1, Oak Ridge National Laboratory, Oak Ridge, TN. 43 p. Available online at http://web.ornl.gov/info/reports/1988/3445602823407.pdf.

THOMPSON, N. 1981. Modelling the field drying of hay. *J. Agric. Sci. Camb.* 97:241–260. doi:10.1017/S0021859600040685.

US DEPARTMENT OF ENERGY. 2011. *U.S. billion-ton update: Biomass supply for a bioenergy and bioproducts industry*, Perlack, R.D., and B.J. Stokes (leads). ORNL/TM-2011/224, Oak Ridge National Laboratory, Oak Ridge, TN. 227 p. Available online at https://www1.eere.energy.gov/bioenergy/pdfs/billion_ton_update.pdf.

WELTY, J., C. WICKS, R. WILSON, AND G. RORRER. 2008. *Fundamentals of momentum, heat, and mass transfer*, 5th ed. John Wiley & Sons, Hoboken, NJ. 711 p.

ZAMORA-CRISTALES, R., J. SESSIONS, K. BOSTON, AND G. MURPHY. 2015. Economic optimization of forest biomass processing and transport in the Pacific Northwest USA. *For. Sci.* 61(2):220–234. doi:10.5849/forsci.13-158.